

# INTERNATIONAL JOURNAL OF CURRENT RESEARCH IN CHEMISTRY AND PHARMACEUTICAL SCIENCES

(p-ISSN: 2348-5213; e-ISSN: 2348-5221)  
www.ijrcps.com



Research Article

## THIADIAZOLE DERIVATIVES AS CORROSION INHIBITORS FOR COPPER-NICKEL ALLOY IN COOLING WATER SYSTEMS

<sup>1</sup>K. CHADRASEKARAN, <sup>2</sup>BANGARU SUDARSAN ALWAR AND <sup>1</sup>R.RAVICHANDRAN\*

<sup>1</sup>Post Graduate & Research Department of Chemistry, Dr.Ambedkar Government Arts College (Autonomous), Chennai – 600 039, India.

<sup>2</sup>Post Graduate & Research Department of Chemistry, D.G. Vaishnav College (Autonomous), Chennai – 600 106, India.

Corresponding Author: varmaravi1965@rediffmail.com

### Abstract

The influence of 2-amino-5-methyl-1,3,4-thiadiazole(AMTD) and 2-amino-5-(methylthio)-1,3,4-thiadiazole(AMTTD) on the corrosion of copper-nickel alloy in natural sea water has been studied using techniques such as weight loss, potentiostatic current transient, potentiodynamic polarization and electrochemical impedance spectroscopic techniques. Polarization studies clearly indicated that the thiadiazole derivatives behave as mixed type inhibitors for copper-nickel alloy in natural sea water. It suppresses the cathodic and anodic reaction rates and it renders the open circuit potential to more noble directions. Measurements of values of charge transfer resistance (Rct) and the double layer capacity (Cdl) have been carried out. Accelerated leaching studies revealed that the inhibitors control the dissolution of copper and nickel in the alloy. The morphology of the Cu-Ni alloy after corrosion in the presence and absence of the thiadiazole derivatives was examined using scanning electron microscopy (SEM).

**Keywords:** copper-nickel alloy, SEM, thiadiazole derivatives, sea water, ICP-AES

### Introduction

Copper and its alloys are widely used in industry because of their excellent electrical and thermal conductivity and are often used in heating and cooling system [Ravichandran et al., 2004]. Copper alloys are used as tubing material for condensers and heat exchangers in various cooling water systems [Quraishi et al., 2000]. Copper-nickel alloys are widely used for marine applications due to their excellent resistance to seawater corrosion, high inherent resistance to biofouling and ease of fabrication. They have provided reliable service for several decades whilst offering effective solutions to today's technological challenges. Copper-nickel alloy is susceptible to a corrosion process known as denickelification [Chandrasekaran et al., 2014]. One of the most important methods in corrosion protection is the utilization of organic inhibitors. Many mechanisms have been proposed for the inhibition of metal corrosion by organic inhibitors which take place

via adsorption and/or hydrogen evolution, which results in a considerable decrease in the corrosion rate. Particularly, on the metal surface [Rozenfeld, 1981, Drazic et al., 1989]. The adsorption process leads to an effective blocking of the active sites of metal dissolution. Heterocyclic organic compounds containing nitrogen, sulphur and/or oxygen atoms are often used to protect metals from corrosion. Among them, azoles have been intensively investigated as effective copper corrosion inhibitors [Geler and Azambuja 2000, Cao et al., 2002]. Thiadiazole, for example, has been studied and found to have excellent inhibition properties in several corrosive environments [Lebrini et al., 2006]. The effectiveness of thiadiazole has been related to the formation of a Cu-Thiadiazole complex film and the film formed is considered to be insoluble and polymeric. Ye et al (1998) studied the structure of the protective film of 1-phenyl-5-mercaptotetrazole (PMTA) formed by pre-

filming the electrode by immersion in the PMTA solution. The film contained a layer of inert, insoluble and long-lasting polymeric Cu (I) complex. These films were probably built over Cu<sub>2</sub>O layer through surface reaction of PMTA and Cu (I) ions. El Warraky (1996) studied the effect of 2-methyl benzimidazole (MBIA) on corrosion behaviour of brass 70Cu/30Zn in deaerated solutions of dilute HCl and acidified 4% NaCl of pH 1.8-2 at different temperatures between 25 and 60°C by the weight loss method. Zhang et al (2004) investigated the protective action of bis-(1-benzotriazolymethylene)-2,5-thiadiazoly)-disulphide on copper in chloride media and concluded that the inhibitors effectively control corrosion. El-Azhar et al (2001) investigated the corrosion inhibition of mild steel by the new class of inhibitors [2,5-bis(n-pyridyl)-1,2,4-thiadiazoles] in acid media using weight loss and electrochemical impedance spectroscopy. Results obtained reveal that these compounds are mixed type inhibitors and behave better in 1M HCl than 0.5M H<sub>2</sub>SO<sub>4</sub>.

In the present investigation, it is proposed to study corrosion protection of cupro- nickel alloy in natural seawater with two thiadiazole derivatives namely 2-amino-5-methyl-1,3,4-thiadiazole and 2-amino-5-(methylthio)-1,3,4-thiadiazole. Weight-loss method and electrochemical studies such as current transient, polarization and impedance spectroscopic techniques were used to assess the inhibition efficiencies of the above compounds. An accelerated leaching study was carried out to find out the concentration of Cu and Ni leached out from the cupro- nickel alloy using ICP-AES. The morphology of the cupro-nickel surface was analyzed using Scanning electron microscopy.

## Experimental details

### Materials

Copper-Nickel (90/10) alloy strips having chemical compositions (wt.%) Cu-89.23%, Ni-9.663%, Mn-0.267%, Fe -0.682%, Pb-0.0594%, Al- 0.0435% and the remainder being other trace amounts of Cr, As, Co and Sr were used. The natural sea water is collected near National Thermal Power Station (NTPC), Ennore, India. The chemical composition of the seawater is analyzed by analytical technique, whose composition is given in Table 1. The pH of the seawater is 6.8. The inhibitors 2-amino-5-methyl-1,3,4-thiadiazole and 2-amino-5-(methylthio)-1,3,4-thiadiazole used is obtained from Sigma-Aldrich and their structures are shown in Fig. 1.

### Methods

#### Weight-loss measurements

The experiments were carried out with Cu/Ni (90/10) alloy specimens of dimension 4 cm x 2.5 cm x 0.2 cm.

The panels were polished mechanically with silicon carbide papers from 120 to 1200 grit. The panels were degreased in acetone, thoroughly washed with double distilled water, dried and weighed. Then the panels were immersed in 300 ml of natural sea water with and without the addition of inhibitors. After immersion for a definite period (45 days) the panels were taken out, washed with distilled water, dried and the changes in weights were noted. Triplicate measurements were carried out for each experiment.

### Potentiostatic current transient techniques

The current transient of alloy specimen as a function of immersion period in the test solution with and without the addition of inhibitors is recorded at a preset potential of -100 mV.

### Polarization studies

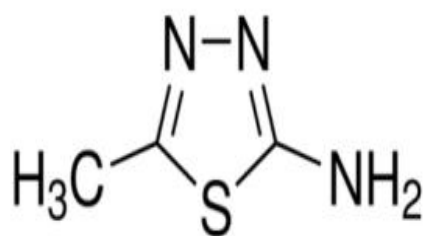
The polarization studies were carried out with Cu/Ni (90/10) alloy specimen having an exposed area of 1cm<sup>2</sup>. The cell assembly consisted of copper-nickel alloy as working electrode, a platinum foil as counter electrode and a saturated calomel electrode (SCE) as a reference electrode with a Luggin capillary bridge. Polarization studies were carried out using a Vibrant potentiostat/galvanostat model No. VSM/CS/30 at a scan rate of 1mV/s.. The degreased working electrode was then inserted into the test solution and immediately cathodically polarized at -1.0 V (SCE) for 15 minutes to reduce any oxides on the Cu/Ni (90/10) alloy [Ravichandran et al., 2005]. The cathodic and anodic polarization curves for alloy specimen in the natural sea water with and without various concentrations of the inhibitors were recorded between -500 to 500 mV at a scan rate of 1 mV/s. The inhibition efficiencies of the compounds were calculated from corrosion current densities using the Tafel extrapolation method.

### Electrochemical Impedance Spectroscopic (EIS) Studies

Electrochemical impedance spectroscopic (EIS) studies were carried out at open circuit potential using a potentiostat/galvanostat (Model PGSTAT 12, AUTOLAB, The Netherlands B.V.) with frequency response analyzer (FRA). Cu/Ni (90/10) alloy specimens with an exposed surface area of 1cm<sup>2</sup> were used as the working electrode. The impedance measurements were carried out at an open circuit potential (OCP), after 1 hr immersion of the Cu/Ni (90/10) electrode in the corrosive medium. The impedance spectra were acquired in the frequency range of 100 KHz – 50 mHz with a 10 mV amplitude sine wave generated by a frequency response analyzer.

**Table 1. Composition of natural sea water**

| Species          | Concentration (mg/ lit) |
|------------------|-------------------------|
| Dissolved oxygen | 0.62                    |
| Chloride         | 29,974                  |
| Sulphate         | 543                     |
| Bicarbonate      | 76                      |
| Phosphate        | 0.59                    |
| Silicate         | 4.52                    |
| Nitrate          | 0.623                   |
| Nitrite          | 0.04                    |



**2-amino-5-methyl-1,3,4-thiadiazole**



**2-amino-5-(methylthio)-1,3,4-thiadiazole**

**Fig. 1. Structures of Inhibitors**

## Solution analysis by inductively coupled atomic emission spectroscopy (ICP-AES)

ICP-AES is a spectroscopic technique with moderate to low detection limits (0.2-100 ppb). Samples are introduced into the system through a nebulizer with argon gas and are dissociated into its constituent atoms and ions. These are then excited by the plasma and a characteristic radiation is emitted for each element as it falls back to the ground state. The intensity of the emission is proportional to the concentration of the element and quantitative analysis is carried out by reference to calibration curves.

The elements detected by ICP-AES in this work are shown below along with the characteristic wavelengths chosen for each element viz Cu and Zn at 325 nm and Ni 352.4 nm respectively. The concentration of Cu and Ni in the electrolytes, after the polarisation experiments in the presence and absence of  $10^{-2}$  M studied inhibitors, was determined by Inductively Coupled Plasma Atomic Emission Spectroscopy (ICPAES). An ICPAES (ARCOS from M/s. Spectro, Germany) was used to measure the amount of dissolution of nickel and copper from the alloy surface. The denickelification factor (n) was calculated using the equation [Chandrasekaran et al.2014].

$$n = \frac{(Ni / Cu)_{soln}}{(Ni / Cu)_{alloy}}$$

where,  $[C_{Ni}/C_{Cu}]_{sol}$  and  $[C_{Ni}/C_{Cu}]_{alloy}$  are the ratios between the concentrations of nickel and copper in the solution and in the alloy respectively.

## Scanning Electron Microscopy

The cupro-nickel alloy surface was prepared by keeping the specimens for an hour in the electrolyte with and without the optimum concentrations of the inhibitors. The cupro-nickel alloy specimens were then washed with distilled water dried and analyzed using SEM. A Philips model XL30SFEG scanning electron microscope with an energy dispersive X-ray analyzer attached was used for surface analysis.

## Results and Discussion

### Weight-loss method

The corrosion rates and inhibition efficiencies of Cu/Ni (90/10) alloy with different concentrations of AMTD and AMTTD in natural sea water at room temperature (30°C) are given in Table 2. The inhibition efficiency increases with increase in concentration of the inhibitors. The maximum IE% of each compound was

achieved at  $10^{-2}$ M, and a further increase in concentration showed only a marginal change in the performance of the inhibitor. The optimum of concentration of the inhibitors was  $10^{-2}$ M and AMTTD was superior to AMTD.

### Mechanism of corrosion inhibition

The dissolution and film formation of copper-nickel alloy in natural sea water takes place via the reactions outlined below.

In the initial corrosion stage, nickel forms NiO as a result of



and copper forms  $Cu_2O$  as a result of



Thus a passive oxide film consisting of both  $Cu_2O$  and NiO covers the surface. However,  $CuCl$  is formed on the surface (in the presence of chloride) by the reaction

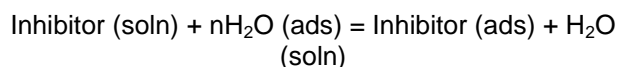


which may ultimately result in the formation of  $CuCl_2$  complex via



The effectiveness of thiadiazole derivatives as corrosion inhibitors for Cu/Ni (90/10) alloy can be gauged from the electrochemical behaviour of cupro-nickel alloy in natural sea water.

The nature of the interaction of inhibitor on the metal surface during corrosion inhibition has been deduced in terms of the adsorption characteristics. In most cases the adsorption of inhibitor from the corrosive medium is a quasi-substitution process.



The thiadiazole derivatives are chemisorbed on the metal surface and that this chemisorbed layer prevents adsorption of oxygen and oxide formation. The protective film is a 1:1 complex of Cu (I) and thiadiazole. The film is probably polymeric, in which thiadiazole bridges two copper atoms via  $N_1$  and  $N_2$  and the aromatic ring is aligned parallel to the metal surface. Formation Cu (II) complexes also can occur, but they do not be protective. Chadwick et al concluded that nickel is also incorporated into the surface film in significant quantities.

Thiadiazole derivatives inhibit the metal by a two-fold mechanism. The chemisorbed film has a hydrophobic backbone that limits the transport of hydrated aggressive ions to the metal surface. Once formed, the film stabilized Cu (I) ions by means of an electronic effect, network formation or both.

It is well known that the inhibitive action of organic compound containing S, N and/or O is due to the formation of a co-ordinate type of bond between the metal and the lone pair of electrons present in the additive. The tendency to form co-ordinate bond and hence the extent of inhibition can be enhanced by increasing the effective electron density at the functional group of the additive. In aromatic or heterocyclic ring compounds, the effective electron density at the functional group can be varied by introducing different substituent in the ring leading to variations of the molecular structure.

Based on the results, both AMTD and AMTTD showed better inhibition efficiencies, due to the presence of heteroatom such as N, O, S and electrons on aromatic nuclei. When compared to AMTD, AMTTD showed highest inhibition efficiency, which may be due to the presence of additional sulphur atom and high molecular weight and possessed by the AMTTD molecule. The higher inhibition efficiency of the organic compounds are due to the basis of donor-acceptor interactions between the electrons of the inhibitor and the vacant d-orbital of copper surface or an interaction of inhibitor with already adsorbed chloride ions.

### Potentiostatic current transient techniques

Figure 2 shows the current-time relationship of the copper-nickel alloy specimen in sea water with and without the optimum concentration of AMTD and AMTTD at the applied potential of -100 mV. During the initial 60 seconds, there was an abrupt decrease in the current and a slower decrease thereafter. After one minute there was no remarkable change in current and a steady value was obtained. Evidently, the intensity of metal dissolution was comparatively low in the presence of inhibitors. Among the inhibitors studied, AMTTD shifted the corrosion current of copper-nickel alloy to a lower value and thus effectively retards the metal dissolution in sea water.

### Potentiodynamic Polarisation Studies

The potentiodynamic polarization curves of copper - nickel alloy in natural seawater in the presence and absence of different concentrations of AMTD and

AMTTD are shown in Figure 3 and 4. Electrochemical kinetic parameters obtained by extrapolation of Tafel

lines are presented in Table 3. The presence of different concentrations of AMTD and AMTTD reduce the anodic and cathodic current densities, and the suppression in current increases as the inhibitor concentration increases; this indicates the inhibiting effects of the two substituted thiadiazole compounds. It can be shown from the table that with increasing inhibitor concentration, corrosion current density ( $I_{corr}$ ) decreases and inhibition efficiency (IE) increases.

The values of cathodic Tafel slope  $b_c$  and anodic Tafel slope  $b_a$  were found to change with increasing inhibitor concentration, which indicated that the inhibitors control both anodic and cathodic reactions. The inhibitors act as relatively mixed type for cupro-nickel alloy (Fouda et al 2010). The shifts of  $E_{corr}$  values towards positive direction are found in the presence of various concentrations of the substituted thiadiazole derivatives in natural seawater. Changes in the corrosion potential ( $E_{corr}$ ) values are due to the result of the competition of the anodic and the cathodic inhibiting reactions of the alloy surface condition.

The inhibition efficiency (IE) was calculated using the following equation (Jayasree and Ravichandran 2013).

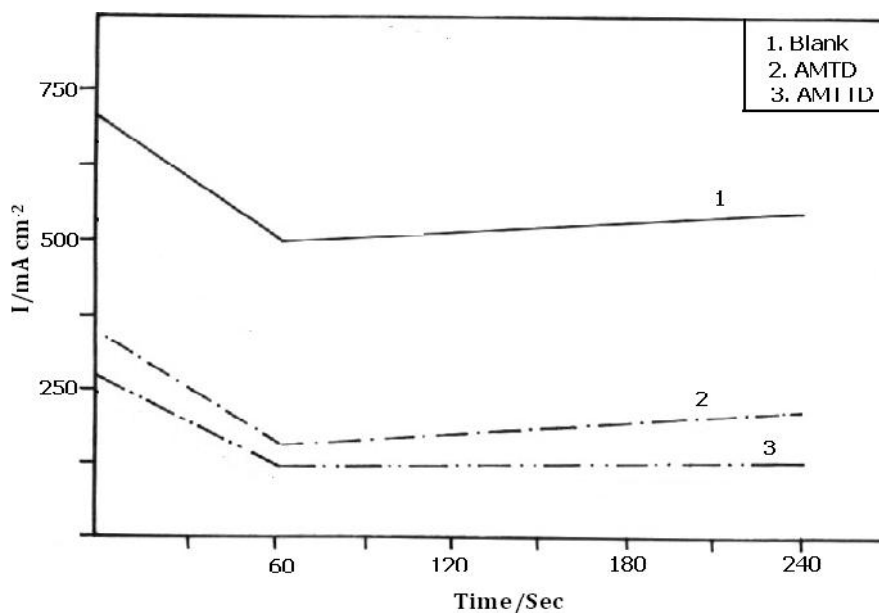
$$I.E.\% = \frac{I_{corr} - I_{corr(inh)}}{I_{corr}} \times 100$$

Where  $I_{corr(inh)}$  and  $I_{corr}$  are corrosion current density in the presence and absence of inhibitors respectively.

The inhibiting property of the studied thiadiazole derivatives is attributed to their ability to chemisorb on the surface of alloy forming few layers of self-assembled films, as sulphur containing compounds are reported to form self-assembled protective layer on the surface of cupro-nickel alloy. The highest inhibition efficiency was observed for AMTTD as it has additional sulfur atom with lone pair of electrons. When compared to AMTD, AMTTD has better efficiency as its molecular size is more and the presence of additional sulphur atom. The values of inhibition efficiency increase with increase in inhibitor concentration, indicating that a higher surface coverage was obtained in a solution with higher inhibitor concentration. It was confirmed that with increase in inhibitor concentration, the corrosion rate

**Table 2.** Inhibition efficiency at different concentrations of AMTD and AMTTD of copper-nickel alloy in natural sea water

| Inhibitor concentration (M) | Corrosion rate $\times 10^{-2}$ (mmpy) | Inhibition efficiency (%) |
|-----------------------------|--|---------------------------|
| Blank                       | 7.694                                  | -                         |
| AMTD                        |  |                           |
| $10^{-5}$                   | 3.392                                  | 55.91                     |
| $10^{-4}$                   | 2.165                                  | 71.86                     |
| $10^{-3}$                   | 1.007                                  | 85.68                     |
| $10^{-2}$                   | 0.642                                  | 91.66                     |
| AMTTD                       |  |                           |
| $10^{-5}$                   | 3.186                                  | 58.60                     |
| $10^{-4}$                   | 1.853                                  | 75.91                     |
| $10^{-3}$                   | 0.814                                  | 89.42                     |
| $10^{-2}$                   | 0.477                                  | 93.80                     |

**Fig. 2** Potentiostatic current transient curves of copper-nickel alloy in sea water containing optimum concentrations of AMTD and AMTTD

decreases. The corrosion inhibition efficiency of AMTTD is higher than that of AMTD.

### Electrochemical Impedance Spectroscopic Studies

The corrosion behaviour of Cu/Ni (90/10) alloy in natural seawater in the presence of AMTD and AMTTD is investigated by the EIS method at 303 K after immersion for 1 h. The Nyquist plots of Cu/Ni (90/10) alloy in natural seawater in the presence and absence of AMTD and AMTTD shown in Figure 5 and 6. The Nyquist plots are significantly changed on addition of inhibitors, the impedance of the inhibited

system increased with inhibitor concentration. The parameters obtained by fitting the equivalent circuit and the calculated inhibition efficiency are listed in Table 4. The impedance spectra of Cu/Ni (90/10) alloy in the presence inhibitors showed a capacitive behavior throughout the measured frequency range. The most pronounced and highest  $R_{ct}$  was observed for AMTTD.  $R_{ct}$  increases with increasing concentration of all inhibitors. It can be seen that by increasing the concentration of thiazole derivatives,  $C_{dl}$  values tend to decrease and the inhibition efficiency increases. The decrease in the  $C_{dl}$  values

**Table 3.** Electrochemical data for corrosion of copper-nickel alloy in natural sea water containing different concentrations of thiadiazole derivatives

| Inhibitor Concentration (M) | $E_{corr}$ (mV vs. SCE) | $b_a$ /mV (dec) <sup>-1</sup> | $b_c$ /mV (dec) <sup>-1</sup> | $I_{corr}$ /~A cm <sup>-2</sup> | Corrosion Rate / mmpy x 10 <sup>-2</sup> | Inhibition Efficiency / % |
|-----------------------------|-------------------------|-------------------------------|-------------------------------|---------------------------------|--|---------------------------|
| Blank                       | -273                    | 69                            | -121                          | 6.23                            | 7.185                                    | -                         |
| AMTD                        |                         |                               |                               |                                 |  |                           |
| 10 <sup>-5</sup>            | -240                    | 95                            | -93                           | 2.61                            | 3.01                                     | 58.11                     |
| 10 <sup>-4</sup>            | -227                    | 114                           | -69                           | 1.58                            | 1.822                                    | 74.64                     |
| 10 <sup>-3</sup>            | -225                    | 130                           | -48                           | 0.64                            | 0.738                                    | 89.73                     |
| 10 <sup>-2</sup>            | -223                    | 146                           | -43                           | 0.34                            | 0.392                                    | 94.54                     |
| AMTTD                       |                         |                               |                               |                                 |  |                           |
| 10 <sup>-5</sup>            | -232                    | 97                            | -90                           | 2.54                            | 2.93                                     | 59.23                     |
| 10 <sup>-4</sup>            | -232                    | 117                           | -66                           | 1.49                            | 1.72                                     | 76.08                     |
| 10 <sup>-3</sup>            | -226                    | 133                           | -47                           | 0.61                            | 0.703                                    | 90.20                     |
| 10 <sup>-2</sup>            | -223                    | 152                           | -39                           | 0.23                            | 0.265                                    | 96.31                     |

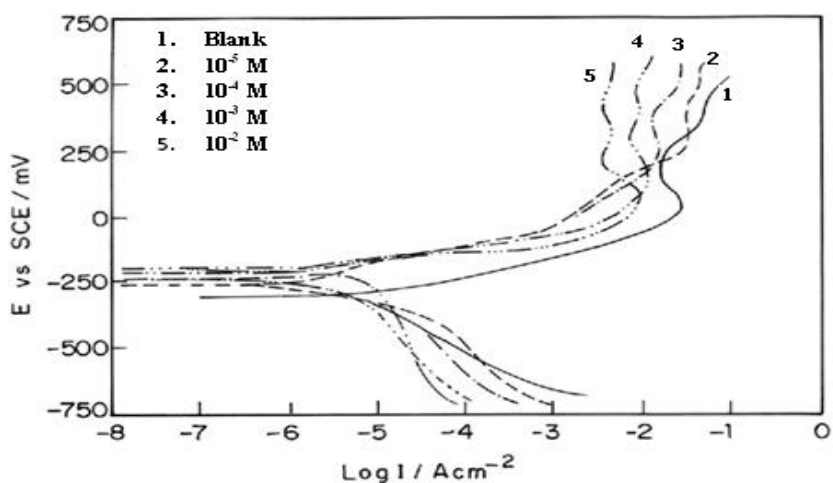


**Fig. 3.** Polarisation curves of copper-nickel alloy in sea water containing different concentrations of AMTD

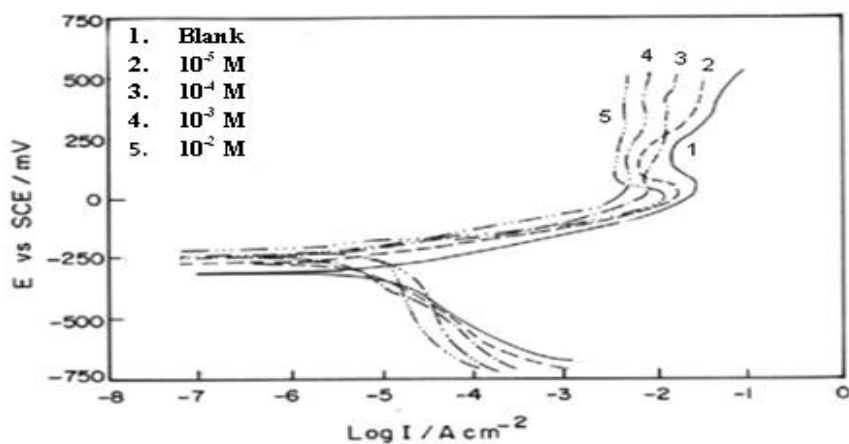


**Fig. 4.** Polarisation curves of copper-nickel alloy in sea water containing different concentrations of AMTTD

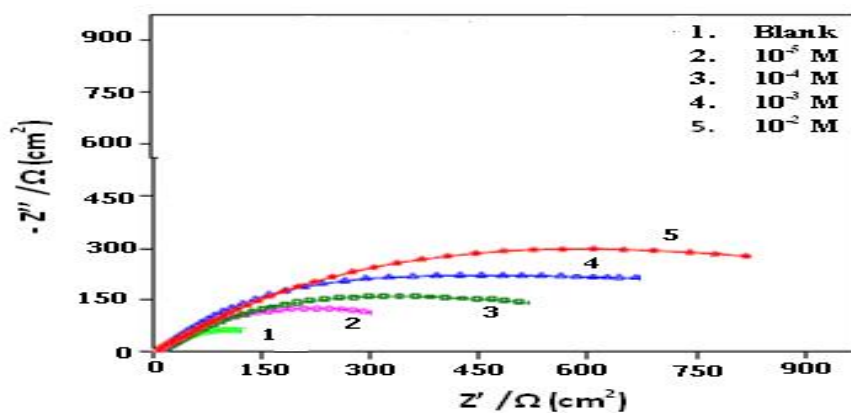


Fig. 5 Nyquist diagrams of copper-nickel alloy in sea water containing different concentrations of AMTD

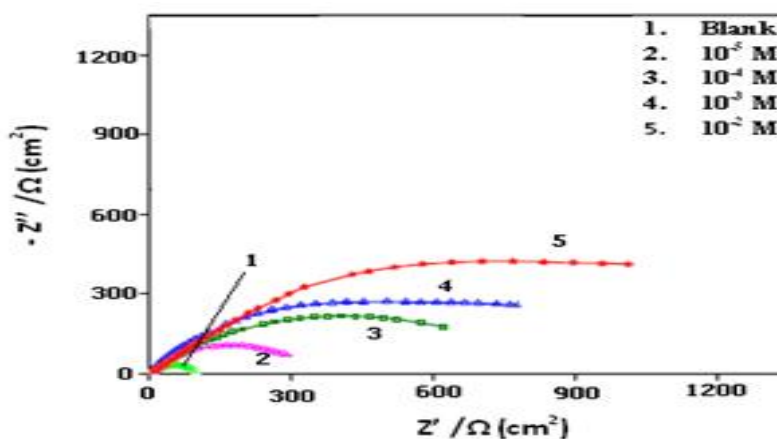


Fig. 6. Nyquist diagrams of copper-nickel alloy in sea water containing different concentrations of AMTTD

Table 4. Impedance Measurements of copper-nickel alloy in natural sea water containing different concentrations of thiadiazole derivatives after 24 hrs immersion.

| Inhibitor Concentration(M) | $R_{ct} \times 10^4$ (ohm $cm^2$ ) | $C_{dl}$ ( $\mu F cm^{-2}$ ) | $R_f$ | $C_f$ | Inhibition Efficiency (%) |
|----------------------------|------------------------------------|------------------------------|-------|-------|---------------------------|
| Blank                      | 0.84                               | 39.47                        | 0.24  | 38.96 | -                         |
| AMTD                       |                                    |                              |       |       |                           |
| $10^{-5}$                  | 2.13                               | 5.38                         | 18.38 | 0.75  | 65.61                     |
| $10^{-4}$                  | 3.60                               | 1.24                         | 135.2 | 0.089 | 77.05                     |
| $10^{-3}$                  | 10.93                              | 0.45                         | 204.7 | 0.052 | 92.31                     |
| $10^{-2}$                  | 16.38                              | 0.13                         | 268.2 | 0.031 | 94.88                     |
| AMTTD                      |                                    |                              |       |       |                           |
| $10^{-5}$                  | 2.57                               | 4.87                         | 22.46 | 0.91  | 66.79                     |
| $10^{-4}$                  | 4.13                               | 0.83                         | 194.3 | 0.076 | 82.61                     |
| $10^{-3}$                  | 12.32                              | 0.19                         | 219.6 | 0.042 | 93.13                     |
| $10^{-2}$                  | 21.65                              | 0.087                        | 289.5 | 0.019 | 96.12                     |

is due to the adsorption of studied inhibitors on the metal surface. The decrease in  $C_{dl}$ , which result from local dielectric constant decrease and/or an increase in the thickness of the electrical double layer, suggest that these molecules act by adsorption on the metal/solution interface. It is clear that  $R_{ct}$  increases and  $C_{dl}$  decreases as the inhibitor concentration increases. The decrease in  $C_{dl}$  could be attributed to the adsorption of the inhibitor, forming protective adsorption layer (Babic-Samardzija et al 2005). A high charge-transfer resistance is associated with a slower corroding system (Hassan et al., 2007). It is clear that the highest values of  $R_{ct}$  observed for AMTTD than AMTD, suggesting the enhanced inhibitor performance. The faradaic resistance that linked to the redox reaction involving corrosion process increases and the faradaic capacitance decreases simultaneously with increase in concentration of all the inhibitors. From this it can be concluded that the corrosion products are less susceptible to redox process with increase in concentration of the inhibitors and give better protection efficiency to cupro-nickel alloy surface. It can be seen that  $R_f$  values increased and  $C_f$  values decreased for all inhibitors. It is attributed to the increase of true surface area which is partly due to the formation of the corrosion products and also to the roughening of electrode surface. The value of resistance and capacitance involved here are very high and it may be related to the redox process taking place at the electrode surface. The inhibition efficiency increased with increase in concentration for all the inhibitors. The comparative study of the corrosion inhibition of thiadiazole-type organic compounds indicates that AMTTD has much significant effect. The investigations proved that the effectiveness of the thiadiazole derivatives as corrosion inhibitors depends on their molecular structure, particularly on their molecular size and electronic effects of the substituent in the molecule. The IE% calculated from EIS show the same trend as those estimated from polarisation measurements.

#### Solution analysis by inductively coupled atomic emission spectroscopy (ICP-AES)

The concentrations of copper and nickel in solutions containing  $10^{-2}$  M of the thiadiazole derivatives after polarisation measurements were determined from inductively coupled plasma atomic emission spectroscopic (ICP-AES) analysis. The denickelification ( $n$ ) factors for cupro-nickel alloy in the absence and presence of  $10^{-2}$  M of AMTD and AMTTD in natural seawater were calculated from the ICP-AES data and the results are given in Table 5. The Concentration of copper and nickel leached out from the alloy in sea water containing optimum concentration of AMTD and AMTTD are shown in Fig. 7 and 8.

The results showed that both copper and nickel were present in the electrolyte in very small quantities and the copper to nickel ratio was found to be lesser than that of the bulk alloy. This is due to the surface barrier arising out of the growth of surface film of inhibitor on the metal surface as well as the corrosion product  $Cu_2O$  and  $NiO$ . It is clear from the table that denickelification was much higher in the absence of inhibitors, while denickelification was much lower in the presence of  $10^{-2}$  M concentration of AMTD and AMTTD. This indicated that the AMTD and AMTTD were able to minimize the dissolution of both Cu and Ni. These values correlate with the corrosion rate and inhibition efficiency obtained by electrochemical methods.

#### Scanning electron microscopy

The surface layer plays a vital role in minimizing the corrosion attack of the aggressive environment. To understand the nature of the surface film in the absence and presence of inhibitors and the extent of corrosion of copper-nickel alloy, the SEM micrographs of the surface were examined. The scanning electron microscopic investigations were carried out in sea water with and without the addition of thiadiazole derivatives at their optimum concentration level. The morphology of the surface of copper-nickel alloy exposed to sea water in the absence and presence of AMTD and AMTTD are shown in Figure 9.

**Table 5.** Effect of optimum concentrations of AMTD and AMTTD on the denickelification of copper-nickel alloy in natural sea water.

| Inhibitors | Solution analysis |          | Denickelification factor (n) | Inhibition Efficiency |        |
|------------|-------------------|----------|------------------------------|-----------------------|--------|
|            | Cu (ppm)          | Ni (ppm) |                              | Cu (%)                | Ni (%) |
| Blank      | 0.946             | 12.36    | 117.71                       | -                     | -      |
| AMTD       | 0.077             | 0.76     | 91.14                        | 91.86                 | 93.85  |
| AMTTD      | 0.062             | 0.52     | 77.44                        | 93.45                 | 97.25  |

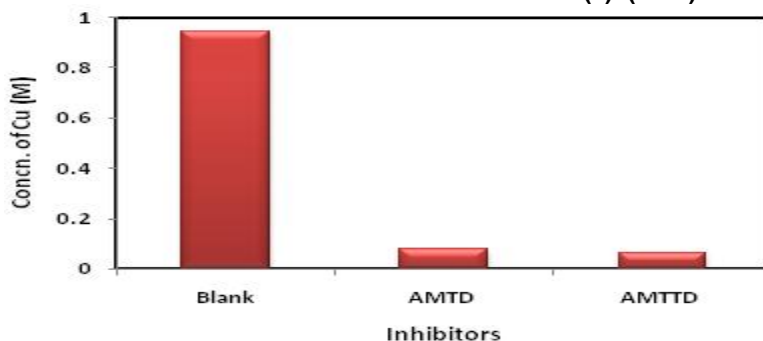


**Fig. 7.** Concentration of copper leached out in sea water containing optimum concentration of AMTD and AMTTD

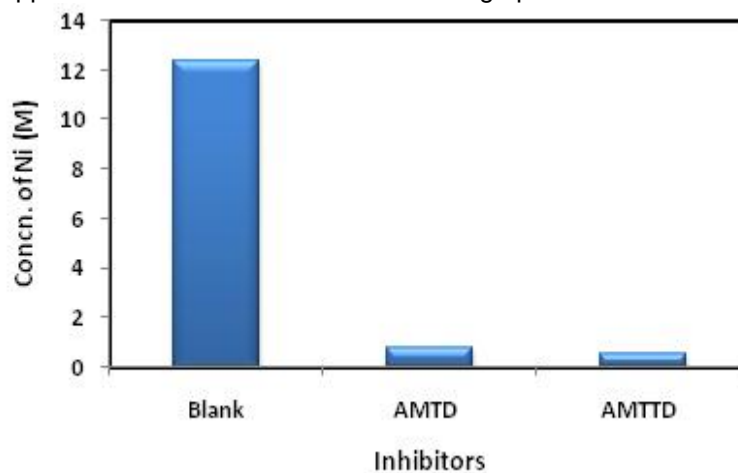


**Fig. 8.** Concentration of nickel leached out in sea water containing optimum concentration of AMTD and AMTTD

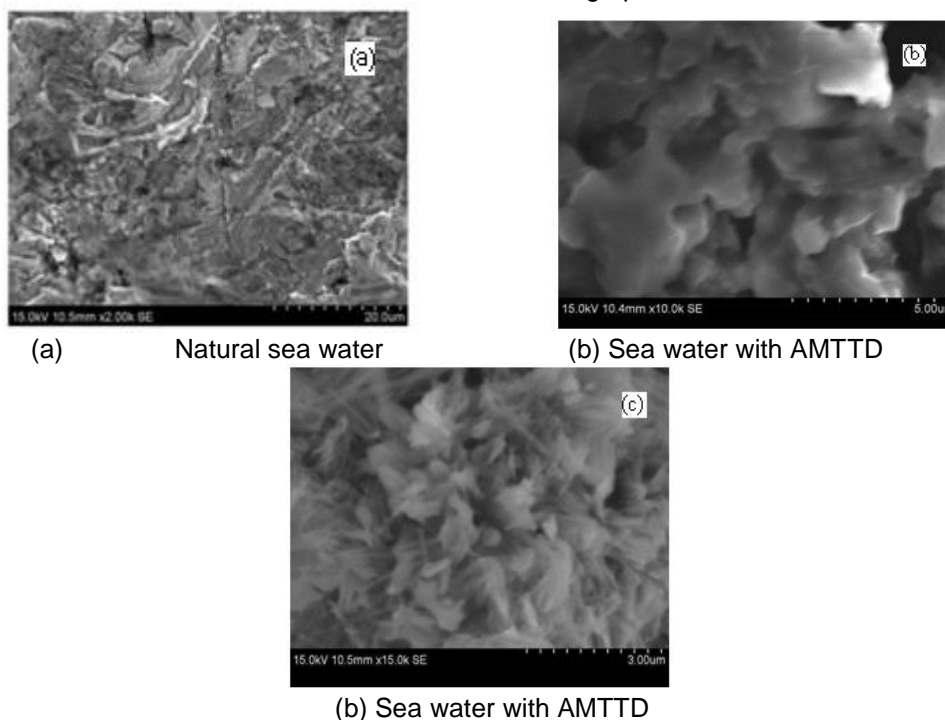


**Fig.9.** SEM micrographs of copper-nickel alloy immersed in natural sea water with and without thiadiazole derivatives

SEM micrograph of the alloy surface exposed to sea water (Figure 9a) showed that the surface was covered by corrosion products mainly consisting of oxides and chlorides. The layer is largely porous in nature and thus anodic dissolution of metals takes place at pores. The SEM micrographs for the alloy exposed to optimum concentration of AMTD in sea water (Figure 9 (b)), revealed that the chemisorbed layer of AMTD blocks the porous oxide layer at the bottom and thus form a compact surface film to provide better corrosion inhibition for copper-nickel alloy in sea water. In the presence of AMTTD, the SEM micrograph (Figure 9(c)) revealed the growth of a film adsorbed on the alloy surface, which was responsible for the corrosion inhibition.

## Conclusion

1. The investigated thiadiazole derivatives show good inhibition efficiencies in natural sea water.
2. The inhibition efficiencies calculated from impedance measurement show the same trend as those observed from polarisation results. The inhibition is due to the formation of an insoluble stable film through the process of complexation of the organic molecules on the metal surface.
3. The dissolution of copper and nickel in the presence of thiadiazole derivatives are low compared to the blank.
4. Scanning electron microscopy clearly proves that the inhibition is due to the formation of an insoluble stable film through the process of complexation of the organic molecules on the metal surface.
5. A combination of electrochemical methods and surface examination techniques are used to investigate the protective film and explain the mechanistic aspects of corrosion inhibition.

## References

Babic Samardzija, K., Khaled, K. F. and Hackerman N. "Investigation of the inhibiting action of O-, S- and N- dithiocarbamate (1, 4, 8, 11-tetraazacyclotetradecane) cobalt (III) complexes on the corrosion of iron in HClO<sub>4</sub> acid", *Appl. Surf. Sci.*, Vol. 240, pp. 327-340, 2005.

Chandrasekaran K, Jayasree A.C, Bangaru Sudarsan Alwar and Ravichandran R, Protective effect of N-

s[(benzylidene hydrazino)-propyl]- benzotriazole and N-[(4-oxo-2-phenyl-1,3-thiazolidineimino)-propyl]-benzotriazole for the control of corrosion of Cu-Ni (90/10) alloy in Sea water, *Elixir Corrosion*, 69 (2014) 22941-22946.

Cao, P. G., Yao, J. L., Zheng, J. W., Gu, R. A. and Tian, Z. Q. "Comparative study of inhibition effects of benzotriazole for metals in neutral solutions as observed with surface-enhanced raman spectroscopy", *Langmuir*, Vol. 18, pp. 100-114, 2002.

Drazic, in: J.O' D.M. Bockers M, White R.E, Canway B.E, (Eds.), *Modern Aspect of Electrochemistry*, Vol. 19, Plenum Press, New York, 1989.

El Azhar M., Mernari B., Traisnel M., Bentiss F. and Lagrenee M. (2001), 'Corrosion inhibition of mild steel by the new class of inhibitors [2,5-bis(n-pyridyl)-1,3,4-thiadiazoles] in acidic media', *Corros. Sci.*, Vol. 43, pp. 2229-2238.

El Warraky, A., El Shayeb, H. A. and Sherif E S. M. "Pitting corrosion of copper in chloride solutions", *Anti-Corros. Method M.*, Vol. 51, pp. 52-61, 2004. 164

El Warraky, A. A. "Dissolution of brass 70/30 (Cu/Zn) and its inhibition during the acid wash in distillers", *J. Mat. Sci.*, Vol. 31, pp. 119-127, 1996.

Fouda, A. S., Mostafa, H. A. and El-Abbasy, H. M. "Antibacterial drugs as inhibitors for the corrosion of stainless steel type 304 in HCl solution", *J. Appl. Electrochem.*, Vol. 40, pp. 163-173, 2010.

Geler, E. and Azambuja, D. S. "Corrosion inhibition of copper in chloride solutions by pyrazole", *Corros. Sci.*, Vol. 42, pp. 631-643, 2000.

Hassan, H. H., Abdelghani, E. and Amin, M. A. "Inhibition of mild steel corrosion in hydrochloric acid solution by triazole derivatives: Part I. polarization and EIS studies", *Electrochim. Acta.*, Vol. 52, pp. 6359-6366, 2007.

Jayasree, A. C. and Ravichandran, R. Corrosion Inhibition of new class substituted benzotriazoles on the brass-mm55 in artificial sea water, *Asian Journal of Science and Technology*, Vol. 4, Issue 11, pp.212-219, November, 2013.

Jayasree A.C, Chandrasekaran K , Ramalakshmi N and Ravichandran R 'Evaluation of New Class of benzotriazoles derivatives as corrosion inhibitor for brass-mm55 in natural sea water by electroanalytical techniques, *International Journal of Current Research in Chemistry and Pharmaceutical Sciences* , Vol. 1 Issue: 6 2014, pp. 77-86.

Lebrini, M., Bentiss, F., Vezin, H. and Lagrenee, M. "The inhibition of mild steel corrosion in acidic solutions by 2, 5-bis (4-pyridyl)-1, 3, 4- thiadiazole:

- structure–activity correlation”, *Corros. Sci.*, Vol. 48, pp. 1279-1291, 2006.
- Lebrini, M., Lagrenee, M., Traisnel, M., Gengembre, L., Vezin, H. and Bentiss F. “Enhanced corrosion resistance of mild steel in normal sulphuric acid medium by 2, 5-bis (n-thienyl)-1, 3, 4-thiadiazoles: Electrochemical, x-ray photoelectron spectroscopy and theoretical studies”, *Appl. Surf. Sci.*, Vol. 253, pp. 9267-9276, 2007.
- Quraishi, M. A., Farooq, I. H. and Saini, P. A. “Inhibition of dezincification of 70-30 brass by amino alkyl mercaptotriazoles”, *Br. Corros. J.*, Vol. 35, pp. 78-80, 2000.
- Ravichandran R., Nanjundan S. and Rajendran N. (2004b), ‘Effect of benzotriazole derivatives on the corrosion and dezincification of brass in neutral chloride solution’, *J. Appl. Electrochem.* Vol. 34, pp.1171-1176.
- Ravichandran R. and Rajendran N. (2005), ‘Influence of benzotriazole derivatives on the dezincification of 65-35 brass in sodium chloride solution’, *Appl. Surf. Sci.*, Vol. 239, pp. 132-142.
- Rozenfeld I.L., *Corrosion Inhibitors*, McGraw-Hill, New York, 1981, p. 327.
- Ye, X. R., Xin, X. Q., Zhu, J. J. and Xue, Z. L. “Coordination compound films of 1-phenyl-5-mercaptotetrazole on copper surface”, *Appl. Surf. Sci.*, Vol. 135, pp. 307-317, 1998.
- Zhang, D., Gao, L. and Zhou, G. “Inhibition of copper corrosion by bis-(1- benzotriazolymethylene)-(2,5-thiadiazoly)-disulphide in chloride media”, *Appl. Surf. Sci.*, Vol. 225, pp. 287-293, 2004.